Earth Planets Space, **65**, 1109–1116, 2013

Clustering of far-infrared galaxies in the AKARI All-Sky Survey North

A. Pollo[1,2], T. T. Takeuchi[3], A. Solarz[3], P. Rybka[3], T. L. Suzuki[3], A. Pępiak[2], and S. Oyabu[3]

[1]*National Centre for Nuclear Research, Hoża 69, 00-681 Warsaw, Poland*
[2]*Astronomical Observatory of the Jagiellonian University, Orla 171, 30-001 Cracow, Poland*
[3]*Division of Particle and Astrophysical Science, Nagoya University, Furo-cho, Chikusa-ku, Nagoya 464-8602, Japan*

(Received December 17, 2012; Revised May 26, 2013; Accepted June 18, 2013; Online published October 24, 2013)

We present the measurements of the angular two-point correlation function for AKARI 90-μm point sources, detected outside the Milky Way plane and other regions characterized by high Galactic extinction in the northern Galactic hemisphere, and categorized as extragalactic sources according to our far-infrared-color based criterion. Together with our previous work (Pollo *et al.*, 2013) this is the first measurement of the large-scale angular clustering of galaxies selected in the far-infrared after IRAS. We present the first attempt to estimate the spatial clustering properties of AKARI All-Sky galaxies and we conclude that they are mostly a very nearby ($z \leq 0.1$) population of moderately clustered galaxies. We measure their correlation length $r_0 \sim 4.5\ h^{-1}$ Mpc, which is consistent with the assumption that the FIS AKARI All-Sky surveys observes mostly a nearby star-forming population of galaxies.

Key words: Galaxies, clustering, large-scale structure, dust, infrared, cosmology.

1. Introduction

In the framework of modern observational cosmology, it is widely assumed that all large-scale structure of the Universe is the result of gravitational instability. In the hierarchical scenario of structure formation, galaxies formed and evolved inside dark matter halos, which grew under the effect of gravity, starting from tiny inhomogeneities in the primordial density field (see, e.g. White and Rees, 1978). The imprint of the primordial distribution of inhomogeneities, although distorted, should be still preserved in the distribution of nowadays galaxies. Therefore, analysis of galaxy clustering is crucial to an understanding of the evolution of the underlying dark matter field. However, understanding the bias between the distribution of galaxies and the underlying dark matter density field is not an easy task, since it depends strongly on galaxy properties, and this dependence evolves and changes with cosmic time.

To make a census of all possible types of galaxies, surveys at different wavelengths have been made in the past. In particular, infrared (IR) galaxies have played an important role. The first reason was statistical, since the Infrared Astronomical Satellite (IRAS: Neugebauer *et al.*, 1984) has resulted in a great amount of data, and the IRAS Point Source Catalog (PSC) provided a big homogeneous dataset of galaxies, which has drastically driven statistical studies. Early studies were based on the angular correlation (Meiksin and Davis, 1986; Rowan-Robinson and Needham, 1986; Lahav *et al.*, 1990; Liu *et al.*, 1994). Later, various IRAS redshift surveys (e.g., Babul and Postman, 1990; Rowan-Robinson *et al.*, 1991; Strauss *et al.*, 1992; Fisher *et al.*, 1995; Saunders *et al.*, 2000) have resulted in tremendous progress in the analysis of the spatial distribution and clustering of IRAS galaxies (e.g., Efstathiou *et al.*, 1990; Saunders *et al.*, 1992; Hamilton, 1993; Fisher *et al.*, 1994; Peacock, 1997). There was also a theoretical reason to treat the IRAS data with a particular interest: in many of these studies, IR galaxies were treated as a tracer of the total baryonic mass contained in galaxies, explicitly or implicitly.

However, this assumption was found not to be completely correct, when it was pointed out that that the amount of dust in galaxies is not always strongly correlated to their stellar mass (e.g., Iyengar *et al.*, 1985; Tomita *et al.*, 1996). Indeed, IRAS galaxies are significantly biased with respect to optical ones (e.g., Babul and Postman, 1990; Lahav *et al.*, 1990; Peacock and Dodds, 1994). Today, we consider IR emission from galaxies to be a good tracer of star-formation activity (e.g., Buat *et al.*, 2007; Takeuchi *et al.*, 2010; Murphy *et al.*, 2011). The large-scale structure of dusty galaxies corresponds then to the star-formation density field in galaxies. This is important, since it may allow us to trace the relation between dark matter density and star-formation activity at different epochs (e.g., Małek *et al.*, 2010; Amblard *et al.*, 2011).

This view has been supported in recent years by numerous studies of the clustering of infrared galaxies, mainly in deep surveys, but more restricted in area, at scales up to a few degrees. Gonzalez-Solares *et al.* (2004) estimated the angular correlation function of ISO 15-μm galaxies in the European Large-Area Infrared Space Observatory (ELAIS) S1 survey. From ISO deep surveys, Matsuhara *et al.* (2000) and Lagache and Puget (2000) performed a power spectrum analysis of the diffuse far-infrared (FIR) background and discovered fluctuations which were attributed to the large-scale clustering of dusty galaxies. More recently, the angu-

doi:10.5047/eps.2013.06.004

lar clustering analysis of Spitzer surveys (e.g., Oliver *et al.*, 2004; de la Torre *et al.*, 2007; Gilli *et al.*, 2007; Magliocchetti *et al.*, 2008), based mainly on mid-infrared (MIR) data, has been performed. Now, thanks to large space facilities, such as Herschel and Planck, results from longer wavelengths start to appear (e.g., Maddox *et al.*, 2010; Cooray *et al.*, 2010; Amblard *et al.*, 2011; Magliocchetti *et al.*, 2011; Planck Collaboration *et al.*, 2011). With the data from the WISE satellite (Wright *et al.*, 2010) we may soon hope for the all-sky measurement of MIR galaxies.

After many years since IRAS, the advent of AKARI (ASTRO-F) opened new possibilities to explore the whole sky in the far infrared (Murakami *et al.*, 2007). The primary purpose of the AKARI mission was to provide second-generation infrared (IR) catalogs to obtain a better spatial resolution and a wider spectral coverage than the IRAS catalog. All-sky surveys and some pointed deep observations have been made by AKARI.

Some related works on the AKARI Deep Field-South (ADF-S) have been published: Małek *et al.* (2010) have performed an attempt to identify the FIR-bright extragalactic sources and used their correlation function to estimate the limitations of the completeness of the sample due to source confusion, while Matsuura *et al.* (2011) measured the power spectrum of the cosmic infrared background (CIB) in the ADF-S, providing a new upper limit for the clustering properties of distant infrared galaxies and any diffuse emission from the early universe which might have contributed to the CIB.

Pollo *et al.* (2013) presented the first measurement of the angular correlation function for FIR-selected extragalactic sources from the AKARI All-Sky Survey. In the present paper, which may be regarded as an extension of this work, we present the first estimations of the spatial parameters of the FIR galaxy clustering based on the FIS AKARI All-Sky Survey data from the northern hemisphere.

This paper is organized as follows: in Section 2, we present the selection of data used for this analysis. In Section 3, we present and discuss the properties of the spatial correlation function, based on the Limber inversion of the angular correlation function, of selected AKARI sources. We present our conclusions in Section 4.

2. Data

2.1 AKARI

AKARI was a Japanese astronomical satellite aimed at performing various large-area surveys at IR wavelengths, from near- to far-infrared (NIR to FIR), with a wavelength coverage of 2–160 μm, as well as pointed observations.[1] AKARI was equipped with a cryogenically cooled telescope of 68.5-cm aperture diameter and two scientific instruments, the Far-Infrared Surveyor (FIS; Kawada *et al.*, 2007) and the Infrared Camera (IRC; Onaka *et al.*, 2007).

2.2 AKARI all-sky surveys

Among the most significant astronomical observations performed by AKARI is an all-sky survey with FIS and IRC; it is referred to as the AKARI All-Sky Survey. It is the second ever all-sky survey performed at FIR, after IRAS. The FIS scanned 96% of the entire sky more than twice in the 16 months of the cryogenic mission phase. In March 2010, the AKARI/FIS Bright Source Catalogue v.1.0 was released to the scientific community. It contains, in total, 427071 point sources measured at 65, 90, 140, 160 μm. Hereafter, we use the notation S_{65}, S_{90}, S_{140} and S_{160} for flux densities in these bands.

The position accuracy of the FIS sources is 8″, since the source extraction is made with grids of this size. The effective size of the point spread function of AKARI FIS in FWHM is estimated to be $37 \pm 1''$, $39 \pm 1''$, $58 \pm 3''$, and $61 \pm 4''$ at 65 μm, 90 μm, 140 μm, and 160 μm, respectively (Kawada *et al.*, 2007). An additional noise factor to be considered is the source confusion: however, in the case of the AKARI data the source confusion limit is estimated to be generally fainter than the detection limit (Jeong *et al.*, 2005, 2006). The flux errors are not estimated for each individual source, but instead they are estimated, in total, to be 35%, 30%, 60%, and 60% at 65 μm, 90 μm, 140 μm, and 160 μm, respectively (Yamamura *et al.*, 2010).

The AKARI All-Sky Survey, and, in particular, the sample used in this paper for the measurement of the clustering properties of extragalactic sources, differs in many details from its precursor: the IRAS sample. First of all, IRAS samples used for similar studies were based on 60-μm measurements, while the AKARI survey is based on the 90-μm band. The depth of the IRAS survey was estimated to be $S_{60} \geq 0.6$ Jy (Rowan-Robinson and Needham, 1986), while the formal depth of the AKARI FIS All-Sky Survey is $S_{90} \geq 0.2$ Jy at the 3σ detection level. The angular resolution of AKARI is also better: less than 1′ at the longest wavelengths, while the resolution of IRAS was $\sim$2′.

Consequently, the properties of objects observed by AKARI in the All-Sky Survey may differ from those of the IRAS sources: since FIS is sensitive at longer wavelengths than is IRAS, we can expect to find objects created from cooler dust, which were difficult to detect by IRAS. Consequently, the clustering properties of galaxies selected from the AKARI FIS catalogs can also be different from those of the corresponding IRAS galaxies.

2.3 Selection of extragalactic sources

As mentioned before, the complete FIS All-Sky Survey contains 427071 point sources. Since the primary detection was performed at 90 μm, all sources have a flux measurement at least at this band.

Further analysis is based on the same sample as selected by Pollo *et al.* (2013), i.e. we restrict ourselves to the area of low contamination from the Galactic FIR emission ($I_{100} \leq 5$ MJy sr^{-1}) measured from the Schlegel maps (Schlegel *et al.*, 1998). Such a procedure enables the avoidance of contamination by sources from the Galactic plane and Galactic cirrus emission.

Because of the inhomogeneity of the results for the northern and southern Galactic hemispheres, found by Pollo *et al.* (2013), we restrict the analysis presented here to sources from the northern hemisphere.

In Pollo *et al.* (2010), we have presented a method to classify the AKARI sources in the color-color diagrams only from FIS bands. In order to be able to apply this method

[1]Detailed information on the AKARI project, instruments, data and important results can be found via URL: http://www.ir.isas.ac.jp/ASTRO-F/index-e.html.

Table 1. Statistics of the identified/unidentified sources in four subsamples with different flux density S_{90} in the AKARI All-Sky Survey North.

limiting S_{90} [Jy]	Number of galaxies	Percentage of unidentified sources	Percentage of stars among identified sources
0.2	8472	16%	9%
0.5	5493	10%	9%
1.0	2233	6%	12%
1.5	1282	3%	15%

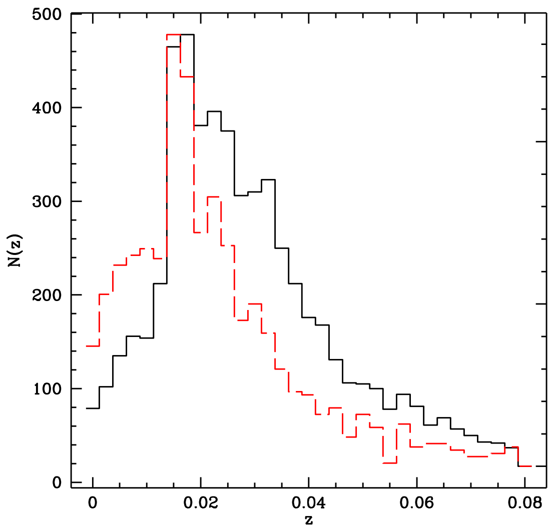

Fig. 1. Renormalized histograms of redshifts z of two samples of the AKARI FIS sources from the northern hemisphere. The solid line corresponds to the "full" sample with $S_{90} \geq 0.2$ Jy, while the dashed line corresponds to the sources from the brightest sample with $S_{90} \geq 1.5$ Jy. Numbers on the left vertical axis correspond to the $S_{90} \geq 0.2$ Jy case, while numbers on the right vertical axis correspond to the $S_{90} \geq 1.5$ Jy sample.

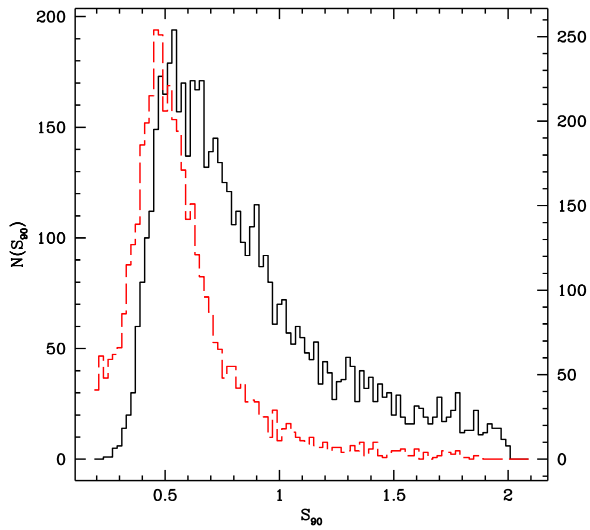

Fig. 2. Renormalized histograms of S_{90} fluxes of the AKARI FIS sources from the northern hemisphere: the solid line corresponds to the sample of identified galaxies with known redshifts, while the dashed line corresponds to the sources identified as galaxies but whose redshift is not known from the literature. Numbers on the left vertical axis correspond to the sample with known redshifts, while numbers on the right vertical axis correspond to the sample without known redshifts.

to select candidates for extragalactic sources in the following analysis, we further restrict ourselves only to sources which were detected at least at 65 μm, 90 μm and 140 μm, with an additional condition of the high quality flag of S_{90} ($f_{90} = 3$, meaning sure detection and secure flux measurement). These conditions were chosen to assure a reasonably high quality of the data, but keeping the numbers of sources used for the subsequent analysis possibly high.

In order to assure a good quality of AKARI photometric measurements, we additionally masked the data, restricting ourselves only to those parts of the sky which were scanned by AKARI at least three times.

Then, we applied our color-based method to select candidates for the extragalactic sources in the low-extinction area. As a result, 8472 objects from the northern Galactic hemisphere were classified as extragalactic sources, while 541 sources were classified as stars. According to Pollo *et al.* (2010), the expected contamination of the extragalactic population by stars is ~4%, while the risk of a galaxy being misidentified as a star is ~17%. However, these errors were estimated for a sample constructed without any restriction for the quality of the flux measurements. Further, some tests (Rybka *et al.*, 2012, 2013) have shown that using only high-quality flags improves these errors significantly; and while some of the Galactic sources remain classified as extragalactic—this applies, for example, to planetary nebulae, due to their intrinsic properties—the risk of misclassification of a galaxy as a star decreases to ~2–3%. Then, given our selection criteria, we expect the contamination of both Galactic and extragalactic groups classified by our algorithm, to be of the order of 2–4%.

This result is supported by tests based on a sample of AKARI All-Sky Survey sources identified in public databases, in a similar way as used in Pollo *et al.* (2010). The counterpart from the literature was searched in a radius of 40″ centered on each AKARI FIS source. In the cases when multiple counterparts were found, in principle the closest one was chosen. However, such cases underwent a more detailed manual scrutiny; for example, if the first counterpart was a very faint Milky Way star and the next, and almost equally close, one was a bright nearby galaxy—we assumed it was rather a galaxy which was a source of the FIR emission and that the presence of the star was a chance coincidence. Another typical example is the case when the closest counterpart given by databases was a star located in a nearby galaxy—in such cases, we assumed that the galaxy as a whole was a source of the FIR emission. Additionally, the cases of single but very distant (radius ≥20″) counterparts were also manually verified.

The analysis of this sample confirmed that the estimation given above is actually correct. Some details, relevant for the subsamples we use in the next part of this paper, are shown in Table 1. In particular, only ∼16% of sources in the whole sample were unidentified—i.e. without counterparts being found in the public databases—and this percentage decreased to only 3% among the brightest galaxies. The percentage of stars increases with the flux of the subsample from ∼9% to ∼15%. Not unexpectedly, unidentified sources, for which no counterpart could be found, neither in the SIMBAD nor in the NED database, dominate the faint end of the flux distribution.

However, most importantly, for ∼60% of the identified galaxies we could find their redshifts in the NED or SIMBAD public databases, and confirm them in the corresponding literature. Histograms of these redshifts for two cases—the full sample and the bright subsample of galaxies with $S_{90} \geq 1.5$—are presented in Fig. 1. The majority of identified sources are located at very low redshifts, below $z \leq 0.1$, with a median at $z \sim 0.03$, decreasing with the limiting flux of the sample. It is also not surprising—as is seen also from Fig. 2, which compares the flux S_{90} histograms for galaxies with known and unknown redshifts—that, for the fainter sources, the chance of having their redshift measured is significantly lower.

Nevertheless, we decided to use the obtained $N(z)$ as the first guess in the attempt to reconstruct the spatial clustering properties of our sample. However, it should be remembered that whereas our $N(z)$, and the resulting clustering properties, will be fairly accurate for the brightest sample, for the fainter ones our $N(z)$ is restricted to its brighter/closer end, and this has to be taken into account in the interpretation of the results.

3. Angular and Spatial Clustering of AKARI All-Sky Survey Galaxies

3.1 Method

The angular two-point correlation function, $\omega(\theta)$ is defined as the excess probability above random that a pair of galaxies is observed at a given angular separation θ (Peebles, 1980). Similarly to Pollo *et al.* (2013), we adopt the angular version of the Landy-Szalay estimator (Landy and Szalay, 1993), that expresses $\omega(\theta)$ as:

$$\omega(\theta) = \frac{N_R(N_R-1)}{N_G(N_G-1)}\frac{GG(\theta)}{RR(\theta)} - \frac{N_R-1}{N_G}\frac{GR(\theta)}{RR(\theta)} + 1. \quad (1)$$

In this expression, N_G and N_R are the total number (equivalently, the mean density may be used) of objects, respectively, in the galaxy sample and in a catalog of random points distributed within the same survey volume and with the same photometric mask applied as the one used for the real data. $GG(\theta)$ is the number of independent galaxy-galaxy pairs with a separation between θ and $\theta + d\theta$; $RR(\theta)$ is the number of independent random-random pairs within the same interval of separations and $GR(\theta)$ represents the number of galaxy-random pairs.

As has been widely discussed in the literature (see, e.g., Hamilton, 1993; Fisher *et al.*, 1994; Norberg *et al.*, 2009), Poissonian errors usually indicate only the lower limit on the actual errors, since they simply reflect the information related to the statistical properties of the sample. In this paper, for simplicity, we apply the analytic estimation of the expected ensemble errors based on the approach introduced by Mo *et al.* (1992), but generalized for the case of the Landy and Szalay estimator we use in this work.

In practice, both the spatial and angular correlation function are usually well fitted by a power-law model:

$$\omega(\theta) = A_w \theta^{1-\gamma}, \quad (2)$$

with $1-\gamma$ being the slope of the correlation function (γ itself is then the slope of a corresponding spatial correlation function) and A_w is the normalization of the correlation function.

3.2 Extraction of the spatial properties of the correlation function

Knowing the properties of the angular correlation function and, at least, the approximate redshift distribution of sources, $N(z)$, we can obtain the parameters of the corresponding spatial correlation function of our galaxies via Limber's equation (Limber, 1954; see, e.g., Peebles, 1980 for details). If we can reasonably approximate the shape of the angular correlation function by the power law, as it is in our case, the Limber inversion can be performed using the formula (Peebles, 1980; Brodwin, 2004):

$$r_0^{-\gamma} = A_\omega \left(\frac{H_0 H_\gamma}{c} \frac{\int (x(z))^{1-\gamma} E(z) N(z)^2}{[\int N(z) dz]^{-2}} \right), \quad (3)$$

where c is the speed of light, H_γ is a combination of Euler's Γ functions:

$$H_\gamma = \frac{\Gamma(1/2)\Gamma((\gamma-1)/2)}{\Gamma(\gamma/2)}, \quad (4)$$

and $x(z)$ is the cosmology dependent comoving radial distance:

$$x(z) = \frac{c}{H_0} \int \frac{dz}{E(z)}, \quad (5)$$

while

$$E(z) = \sqrt{\Omega_M (1+z)^3 + \Omega_k (1+z)^2 + \Omega_\Lambda}. \quad (6)$$

For the sake of accuracy, in the calculations we assume a flat Λ cold dark matter (CDM) cosmology, with a mass density parameter $\Omega_M = 0.3$ and $\Omega_\Lambda = 0.7$. However, since our sample consists mostly of very nearby galaxies, our results are not very far from those which would be obtained from computations based on a flat cosmology with $\Omega_\Lambda = 0$ and, therefore, our results can be compared—with due caution—to much earlier results from the literature (e.g. based on IRAS).

Correlation lengths r_0 are given in units of $h = H_0/100$ km s^{-1} Mpc^{-1}, where H_0 is the Hubble constant.

In principle, the Limber inversion technique is not completely stable and it depends on the estimation of $N(z)$, especially for narrow redshift bins. Moreover, the Limber equation was derived for the small-angle approximation and should be used only for surveys in which distances of galaxies both in the sky and in the z-space are not too large. Keeping these limitations in mind, we treat it, in this case, only as the first approximation of the spatial clustering properties of AKARI galaxies.

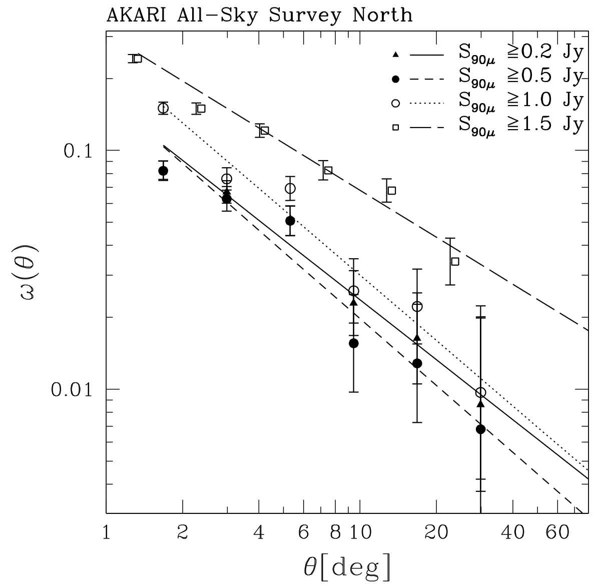

Fig. 3. Angular correlation function in the AKARI All-Sky Survey North—comparison of subsamples with different limits of flux density S_{90}. Points correspond to the measurements in the logarithmic bins and lines show the best power-law fit. Full triangles and the solid line correspond to the whole sample, i.e. $S_{90} > 0.2$ Jy. Full circles and the short-dashed line correspond to the sample with a limit $S_{90} > 0.5$ Jy. Open circles and the dotted line correspond to the sample limited by $S_{90} > 1$ Jy. The brightest sample, $S_{90} > 1.5$ Jy, is shown by open squares and the long-dashed line.

3.3 Spatial clustering of flux density limited samples in the AKARI All-Sky Survey North

The dependence of the clustering properties of AKARI FIS galaxies on their flux density in 90 μm is presented in Fig. 3. The parameters of clustering—angular and spatial—are presented in Table 2. Even if the properties of all subsamples roughly remain consistent with respect to the estimated error bars, a general trend is similar to the one observed in other similar measurements: brighter galaxies are clustered more strongly than fainter ones, and the angular clustering length increases with the limiting flux density. The reversal of this trend, observed for the two faintest samples: limited by $S_{90} > 0.5$ Jy and by $S_{90} > 0.2$ Jy, should rather be attributed to larger systematic errors of the flux measurement of the faintest sources.

3.3.1 Clustering length of AKARI galaxies The derived value of the spatial clustering length, r_0, remains similar, $\sim$4.2–4.8 h^{-1} Mpc, for all the measured subsamples. It can be located between the value of $\sim$4 h^{-1} Mpc estimated for IRAS galaxies (Lahav *et al.*, 1990) and the "canonical" value of 5 h^{-1} Mpc for local bright optically-selected galaxies (Peebles, 1980), and—given the error bars—in most cases, is consistent with both of these values. Broadly speaking, this is consistent with the hypothesis that these galaxies belong to a population of star-forming galaxies and do not reside in the high density, or in the very low density, areas.

As was mentioned before, this value computed from the Limber inversion is relatively sensitive to the accuracy of the assumed $N(z)$. In our case, we can assume that the computed $N(z)$ is fairly accurate since almost all galaxies in this sample are identified and have their redshifts measured.

For the fainter samples, we can reasonably assume that the actual redshift distributions have longer tails towards higher z. The derived $r_0 \sim 4.5\ h^{-1}$ Mpc can then be regarded as the upper limit of the correlation lengths of these samples, since the more realistic galaxy distribution would imply that more galaxy pairs which are close in the sky are, in fact, physically uncorrelated.

One striking feature is a relatively weak dependence of the measured value of r_0 on the observed 90-μm flux. In fact, the luminosity dependence of galaxy clustering is much less clear in the case of the FIR measurements than, for example, in optical surveys. A relatively flat dependence of r_0 on S_{90} can be attributed to the fact that the FIR luminosity of a galaxy is not only a function of the dark halo mass in which the galaxy resides. In addition, it strongly depends on the efficiency of the star-formation processes in a galaxy, and can be related to its specific star formation rate (SSFR). While r_0 should be higher for galaxies with higher halo masses, for actively star-forming galaxies we expect an opposite effect—galaxies with higher SSFR may be less clustered (e.g. Hawkins *et al.*, 2008). The observed weak tendency of r_0 to increase with the observed FIR flux may result from a combination of these two effects.

On the other hand, r_0 measured for our samples is higher than that obtained for local star-forming galaxies selected according to some other star activity tracers. For instance, for local ultraviolet (UV) selected galaxies from the FOCA survey, Heinis *et al.* (2004) found $r_0 = 3.2^{+0.8}_{-2.3}\ h^{-1}$ Mpc, while for local ultraviolet (UV) selected galaxies from the GALEX data, Milliard *et al.* (2007) measured $r_0 = 3.6 \pm 0.6$ Mpc. This difference may be a result of a combination of selection effects related, for example, to the depth of all the analyzed samples. However, the likely explanation is that different tracers tend to favor different types of star-forming galaxies, typically located in haloes of different masses and with different clustering properties.

3.3.2 Clustering slope of AKARI galaxies The slope γ of our AKARI correlation function is similar to that of optically-selected galaxies, but steeper than that of IRAS galaxies ($\gamma \simeq 1.6$–1.7: e.g. Lahav *et al.*, 1990). More recent works show rather controversial results on the slopes of IR-selected galaxies. Gonzalez-Solares *et al.* (2004) presented an angular correlation function of galaxies detected in the ISO ELAIS N1 field. Their power-law slope was $\gamma \sim 2.0$, even steeper than those of optical galaxies. Gilli *et al.* (2007) showed a correlation function of Spitzer MIPS 24-μm-selected galaxies at $z \sim 1$, whose power-law slope is $\sim$1.5. Maddox *et al.* (2010) analyzed the clustering of submillimeter galaxies detected by Herschel in the H-ATLAS survey. They have found a very steep slope of $\gamma \sim 2.0$. There are many other surveys with recent facilities, but most of the analyses assume a fixed value of $\gamma = 1.8$ and we cannot compare our result with them.

However, we should take into account that estimating a slope of the two-point correlation function of IR-selected galaxies may be a subject of some biasing effects. First of all, one has to keep in mind that the values of A_ω (or r_0) are not independent. Secondly, the shape of the correlation function very often cannot be fitted by a power-law func-

Table 2. Clustering properties of four subsamples with different flux density S_{90} in the AKARI All-Sky Survey North.

limiting S_{90} [Jy]	Number of galaxies	Median z	A_w [deg]	r_0 [h^{-1} Mpc]	γ
0.2	8472	0.030	$0.16^{+0.02}_{-0.01}$	4.49 ± 0.74	1.8 ± 0.1
0.5	5493	0.029	0.16 ± 0.02	4.24 ± 0.41	1.9 ± 0.1
1.0	2233	0.022	$0.24^{+0.05}_{-0.04}$	4.44 ± 0.54	1.9 ± 0.2
1.5	1282	0.018	$0.30^{+0.07}_{-0.05}$	4.8 ± 0.36	$1.7^{+0.2}_{-0.1}$

tion perfectly. There are two possible reasons for the deviation from the power-law shape. One is physical—the mass distribution inside dark matter haloes, and, consequently, the distribution of galaxies, is expected to be different than the distribution of dark matter and galaxies on larger scales. This effect is taken into account when the so-called Halo Occupation Distribution models are used to fit the correlation function shape (Peacock and Smith, 2000; Seljak, 2000; Berlind and Weinberg, 2002). The so-called one halo term is often seen as the increase of the clustering power on the small scales, which may result in the total increase of the measured value of γ if these scales are taken into account in the fitting process. In principle, one might expect such an effect from the population of star-forming, and often interacting, galaxies—even if they are not very massive or located in particularly dense environments. However, there exists also a second effect, which is related to the limited resolution of the IR catalogs due to source confusion. This may cause two or more close galaxies to be detected as a single source, and decreases the clustering power measured below the angular scale affected by source confusion. If the fitting of the correlation function shape includes these small scales, the measured value of γ is decreased (see also Małek *et al.*, 2010).

Considering all the possible effects mentioned above, we may try to interpret our results: since our measurement is performed on large scales, omitting the scales where both the one halo term and source confusion may play a significant role, the measured slope remains most similar to that typically found for the optically-selected galaxies.

4. Summary and Conclusions

We present measurements of the angular and spatial clustering of far-infrared galaxies in the AKARI FIS All-Sky Survey. We have measured the angular two-point correlation function for four flux-limited subsamples of 90-μm-selected catalog of galaxies in the northern Galactic hemisphere. Our conclusions are as follows:

(1) Cross-identification with the public catalogs indicates that the sources we identified as extragalactic using the color-color criteria are indeed galaxies, and that at least 60% of them are very nearby galaxies at $z < 0.1$.

(2) The amplitude of the angular correlation function of FIR galaxies rises with an increasing flux density limit of the sources, in accordance with expectations for a sample of relatively nearby galaxies. However, the dependence of the spatial correlation length, measured using the Limber inversion, on the observed flux is rather weak. This is consistent with the hypothesis that FIR luminosities of these galaxies are determined not only by the masses of their dark matter haloes but also by other factors, most likely related to the star-forming processes in them.

(3) The measured slope of the correlation function, $\gamma \sim 1.8$ is steeper than that measured, for example, for IRAS galaxies, which may result from the better angular resolution of AKARI.

(4) For the brightest galaxies we measure, using the Limber inversion, a spatial correlation length $r_0 \sim 4.8$ h^{-1} Mpc. This value lies between the value typically measured for the IR galaxies, for example, in the IRAS sample ($r_0 \sim 4$ h^{-1} Mpc; Lahav *et al.*, 1990), and the typical $r_0 \sim 5$ h^{-1} Mpc measured for optical galaxies (Peebles, 1980) and is consistent with the latter one. This is consistent with the hypothesis that these galaxies belong to a population of star-forming galaxies and do not reside neither in high or very low density areas. Rather, they seem to follow an average density field of galaxies.

(5) The correlation lengths measured for AKARI galaxies are higher than the correlation lengths measured for local star-forming galaxies selected according to their UV observed flux. A possible explanation is that different tracers of star-formation in galaxies favor different populations of star forming galaxies.

Acknowledgments. We would like to thank both referees: Dr. Shuji Matsuura and an anonymous referee for their comments, which helped to improve this paper significantly. This work is based on observations with AKARI, a JAXA project with the participation of ESA. AP, AS, PR and AP have been supported by the research grants of the Polish National Science Centre N N203 51 29 38 and N. 2012/07/B/ST9/04425. This research was partially supported by the project POLISH-SWISS ASTRO PROJECT co-financed by a grant from Switzerland through the Swiss Contribution to the enlarged European Union. TTT has been supported by the Grant-in-Aid for the Scientific Research Fund (23340046 and 24111707) commissioned by the Ministry of Education, Culture, Sports, Science and Technology (MEXT) of Japan. TTT, AS, TLS, and SO have also been partially supported from the Grant-in-Aid for the Global COE Program “Quest for Fundamental Principles in the Universe: from Particles to the Solar System and the Cosmos”, and Strategic Young Researchers Overseas Visits Program for Accelerating Brain Circulation from the MEXT. A. Pępiak has been also supported by the scientific grant from the Dean of the Faculty of Physics, Astronomy and Applied Computer Science of the Jagiellonian University, decision no. DSC/000707/2012.

References

Amblard, A. *et al.*, Submillimetre galaxies reside in dark matter haloes with masses greater than 3×10^{11} solar masses, *Nature*, **470**, 510–512, 2011.

Babul, A. and M. Postman, IRAS galaxies and the large-scale structure in the CfA slice, *Astrophys. J.*, **359**, 280–290, 1990.

Berlind, A. A. and D. H. Weinberg, The halo occupation distribution: Toward an empirical determination of the relation between galaxies and mass, *Astrophys. J.*, **575**, 587–616, 2002.

Brodwin, M., The Canada-France deep fields-photometric redshift survey: An investigation of galaxy evolution using photometric redshifts, PhD thesis, University of Toronto, 2004.

Buat, V. *et al.*, The local universe as seen in the far-infrared and far-ultraviolet: A global point of view of the local recent star formation, *Astrophys. J. Suppl. Ser.*, **173**, 404–414, 2007.

Cooray, A. *et al.*, HerMES: Halo occupation number and bias properties of dusty galaxies from angular clustering measurements, *Astron. Astrophys.*, **518**, L22, 2010.

de la Torre *et al.*, VVDS-SWIRE. Clustering evolution from a spectroscopic sample of galaxies with redshift $0.2 < z < 2.1$ selected from Spitzer IRAC 3.6 μm and 4.5 μm photometry, *Astron. Astrophys.*, **475**, 443–451, 2007.

Efstathiou, G., N. Kaiser, W. Saunders, A. Lawrence, M. Rowan-Robinson, R. S. Ellis, and C. S. Frenk, Large-scale clustering of IRAS galaxies, *Mon. Not. R. Astron. Soc.*, **247**, 10P, 1990.

Fisher, K. B., M. Davis, M. A. Strauss, A. Yahil, and J. Huchra, Clustering in the 1.2-Jy IRAS Galaxy Redshift Survey. I - The redshift and real space correlation functions, *Mon. Not. R. Astron. Soc.*, **266**, 50, 1994.

Fisher, K. B., J. P. Huchra, M. A. Strauss, M. Davis, A. Yahil, and D. Schlegel, The IRAS 1.2 Jy survey: Redshift data, *Astrophys. J. Suppl. Ser.*, **100**, 69, 1995.

Gilli, R., E. Daddi, R. Chary, M. Dickinson, D. Elbaz, M. Giavalisco, M. Kitzbichler, D. Stern, and E. Vanzella, The spatial clustering of mid-IR selected star forming galaxies at $z \sim 1$ in the GOODS fields, *Astron. Astrophys.*, **475**, 83–99, 2007.

Gonzalez-Solares, E. A., S. Oliver, C. Gruppioni, F. Pozzi, C. Lari, M. Rowan-Robinson, S. Serjeant, F. La Franca, and M. Vaccari, Large-scale structure in the ELAIS S1 Survey, *Mon. Not. R. Astron. Soc.*, **352**, 44–48, 2004.

Hamilton, A. J. S., Omega from the anisotropy of the redshift correlation function in the IRAS 2 Jansky survey, *Astrophys. J.*, **406**, L47–L50, 1993.

Hawkins, E., S. Maddox, E. Branchini, and W. Saunders, The clustering of hot and cold IRAS galaxies: The redshift space correlation function, *Mon. Not. R. Astron. Soc.*, **325**, 589–598, 2008.

Heinis, S., M. Treyer, S. Arnouts, B. Milliard, J. Donas, R. Gal, D. C. Martin, and M. Viton, The clustering of ultraviolet-selected galaxies at $z \sim 0.1$, *Astron. Astrophys.*, **424**, L9–L12, 2004.

Iyengar, K. V. K., T. N. Rengarajan, and R. P. Verma, Properties of IRAS galaxies with $B(0)_T$ not greater than approximately 14.5, *Astron. Astrophys.*, **148**, 43–51, 1985.

Jeong, W.-S., H. M. Lee, S. Pak, T. Nakagawa, S. Minn Kwon, C. P. Pearson, and G. J. White, Far-infrared detection limits - I. Sky confusion due to Galactic cirrus, *Mon. Not. R. Astron. Soc.*, **357**, 535–547, 2005.

Jeong, W.-S., C. P. Pearson, H. M. Lee, S. Pak, and T. Nakagawa, Far-infrared detection limits - II. Probing confusion including source confusion, *Mon. Not. R. Astron. Soc.*, **369**, 281–294, 2006.

Kawada, M. *et al.*, The Far-Infrared Surveyor (FIS) for AKARI, *Publ. Astron. Soc. Jpn.*, **59**, 389–400, 2007.

Lagache, G. and J. L. Puget, Detection of the extra-Galactic background fluctuations at 170 μm, *Astron. Astrophys.*, **355**, 17–22, 2000.

Lahav, O., R. J. Nemiroff, and T. Piran, Relative bias parameters from angular correlations of optical and IRAS galaxies, *Astrophys. J.*, **350**, 119–124, 1990.

Landy, S. D. and A. S. Szalay, Bias and variance of angular correlation functions, *Astrophys. J.*, **412**, 64–71, 1993.

Limber, D. N., The analysis of counts of the extragalactic nebulae in terms of a fluctuating density field, *Astrophys. J.*, **117**, 134–144, 1954.

Liu, B., G. Wang, X. Y. Xia, and Z. G. Deng, Two-dimensional analysis of galaxies from IRAS faint sources catalog, *Acta Astrophysica Sinica*, **14**, 207, 1994.

Maddox, S. J. *et al.*, Herschel-ATLAS: The angular correlation function of submillimetre galaxies at high and low redshift, *Astron. Astrophys.*, **518**, L11, 2010.

Magliocchetti, M., M. Cirasuolo, R. J. McLure, J. S. Dunlop, O. Almaini, S. Foucaud, G. de Zotti, C. Simpson, and K. Sekiguchi, On the evolution of clustering of 24-μm-selected galaxies, *Mon. Not. R. Astron. Soc.*, **383**, 1131–1142, 2008.

Magliocchetti, M., *et al.*, The PEP survey: Clustering of infrared-selected galaxies and structure formation at $z \sim 2$ in GOODS-South, *Mon. Not. R. Astron. Soc.*, **416**, 1105–1117, 2011.

Małek, K., A. Pollo, T. T. Takeuchi, P. Bienias, M. Shirahata, S. Mof atsuura, and M. Kawada, Star forming galaxies in the AKARI deep field south: Identifications and spectral energy distributions, *Astron. Astrophys.*, **514**, A11, 2010.

Matsuhara, H. *et al.*, ISO deep far-infrared survey in the "Lockman Hole". II. Power spectrum analysis: Evidence of a strong evolution in number counts, *Astron. Astrophys.*, **361**, 407–414, 2000.

Matsuura, S., M. Shirahata, M. Kawada, T. T. Takeuchi, D. Burgarella, D. L. Clements, W.-S. Jeong, H. Hanami, S. A. Khan, H. Matsuhara, T. Nakagawa, S. Oyabu, C. P. Pearson, A. Pollo, S. Serjeant, T. Takagi, and G. J. White, Detection of the cosmic far-infrared background in AKARI deep field south, *Astrophys. J.*, **737**, 2, 2011.

Meiksin, A. and M. Davis, Anisotropy of the galaxies detected by IRAS, *Astron. J.*, **91**, 191–198, 1986.

Milliard, B., S. Heinis, J. Blaizot *et al.*, Clustering properties of rest-frame UV-selected galaxies. I. The correlation length derived from GALEX data in the local universe, *Astrophys. J. Suppl. Ser.*, **173**, 494–502, 2007.

Mo, H. J., Y. P. Jing, and G. Boerner, On the error estimates of correlation functions, *Astrophys. J.*, **392**, 452–457, 1992.

Murakami, H. *et al.*, The Infrared Astronomical Mission AKARI, *Publ. Astron. Soc. Jpn.*, **59**, S369–376, 2007.

Murphy, E. J. *et al.*, Calibrating extinction-free star formation rate diagnostics with 33 GHz free-free emission in NGC 6946, *Astrophys. J.*, **737**, 67, 2011.

Neugebauer, G. *et al.*, The infrared astronomical satellite (IRAS) mission, *Astrophys. J.*, **278**, L1–L6, 1984.

Norberg, P., C. M. Baugh, E. Gaztañaga, and D. J. Croton, Statistical analysis of galaxy surveys - I. Robust error estimation for two-point clustering statistics, *Mon. Not. R. Astron. Soc.*, **396**, 19–38, 2009.

Oliver, S. *et al.*, Angular clustering of galaxies at 3.6 microns from the Spitzer wide-area onfrared extragalactic (SWIRE) survey, *Astrophys. J. Suppl. Ser.*, **154**, 30–34, 2004.

Onaka, T. *et al.*, The infrared camera (IRC) for AKARI—design and imaging performance, *Publ. Astron. Soc. Jpn.*, **59**, 401, 2007.

Peacock, J. A., The evolution of galaxy clustering, *Mon. Not. R. Astron. Soc.*, **284**, 885–898, 1997.

Peacock, J. A. and S. J. Dodds, Reconstructing the linear power spectrum of cosmological mass fluctuations, *Mon. Not. R. Astron. Soc.*, **267**, 1020, 1994.

Peacock, J. A. and R. E. Smith, Halo occupation numbers and galaxy bias, *Mon. Not. R. Astron. Soc.*, **318**, 1144–1156, 2000.

Peebles, P. J. E., *The Large Scale Structure of the Universe*, Princeton University Press, Princeton, 1980.

Planck Collaboration, Planck early results. XVIII. The power spectrum of cosmic infrared background anisotropies, *Astron. Astrophys.*, **536**, A18, 2011.

Pollo, A., P. Rybka, and T. T. Takeuchi, Star-galaxy separation by far-infrared color-color diagrams for the AKARI FIS all-sky survey (bright source catalog version β-1), *Astron. Astrophys.*, **514**, A3, 2010.

Pollo, A., T. T. Takeuchi, T. L. Suzuki, and S. Oyabu, Clustering of far-infrared galaxies in the AKARI all-sky survey, *Earth Planets Space*, **65**, 273–279, 2013.

Rowan-Robinson, M. and G. Needham, The two-dimensional covariance function for IRAS sources, *Mon. Not. R. Astron. Soc.*, **222**, 611–617, 1986.

Rowan-Robinson, M., W. Saunders, A. Lawrence, and K. Leech, The QMW IRAS galaxy catalogue—A highly complete and reliable IRAS 60-micron galaxy catalogue, *Mon. Not. R. Astron. Soc.*, **253**, 485–495, 1991.

Rybka, P., A. Pollo, and T. T. Takeuchi, Classification schemes and properties of infrared galaxies, *Publ. Korean Astron. Soc.*, **27**, 293–294, 2012.

Rybka, P., A. Pollo, and T. T. Takeuchi, 2013 (in prep.).

Saunders, W., M. Rowan-Robinson, and A. Lawrence, The spatial correlation function of IRAS galaxies on small and intermediate scales, *Mon. Not. R. Astron. Soc.*, **258**, 134–146, 1992.

Saunders, W. *et al.*, The PSCz catalogue, *Mon. Not. R. Astron. Soc.*, **317**, 55–63, 2000.

Schlegel, D. J., D. P. Finkbeiner, and M. Davis, Maps of dust infrared emission for use in estimation of reddening and cosmic microwave background radiation foregrounds, *Astron. Astrophys.*, **500**, 525–553, 1998.

Seljak, U., Analytic model for galaxy and dark matter clustering, *Mon. Not. R. Astron. Soc.*, **318**, 203–213, 2000.

Strauss, M. A., J. P. Huchra, M. Davis, A. Yahil, K. B. Fisher, and J. Tonry, A redshift survey of IRAS galaxies. VII—The infrared and redshift data for the 1.936 Jansky sample, *Astrophys. J. Suppl. Ser.*, **83**, 29–63, 1992.

Takeuchi, T. T., V. Buat, S. Heinis, E. Giovannoli, F.-T. Yuan, J. Iglesias-Páramo, K. L. Murata, and D. Burgarella, Star formation and dust extinction properties of local galaxies from the AKARI-GALEX all-sky surveys. First results from the most secure multiband sample from the far-ultraviolet to the far-infrared, *Astron. Astrophys.*, **514**, A4, 2010.

Tomita, A., Y. Tomita, and M. Saitō, A variation in the present star formation activity of spiral Ggalaxies, *Publ. Astron. Soc. Jpn.*, **48**, 285–303, 1996.

White, S. D. M. and M. J. Rees, Core condensation in heavy halos—A two-stage theory for galaxy formation and clustering, *Mon. Not. R. Astron. Soc.*, **183**, 341–358, 1978.

Wright, E. L. *et al.*, The wide-field infrared survey explorer (WISE): Mission description and initial on-orbit performance, *Astron. J.*, **140**, 1868–1881, 2010.

Yamamura, I., S. Makiuti, N. Ikeda, Y. Fukuda, S. Oyabu, T. Koga, and G. J. White, AKARI/FIS all-sky survey bright source catalogue version 1.0 release note, ISAS/JAXA, 2010.

A. Pollo (e-mail: apollo@fuw.edu.pl), T. T. Takeuchi, A. Solarz, P. Rybka, T. L. Suzuki, A. Pępiak, and S. Oyabu